Bull. Chem. Soc. Ethiop. **2026**, 40(12), 2717-2738.
DOI: https://dx.doi.org/10.4314/bcse.v40i12.15
ISSN 1011-3924
Printed in Ethiopia
Online ISSN 1726-801X
© 2026 Chemical Society of Ethiopia and The Authors

EFFICIENT NANO AND MICRO-CRYSTALLINE CELLULOSE BASED ON DATE PALM KERNEL WASTE EXTRACT: *IN-VITRO* BIOLOGICAL ACTIVITIES

Fahad M. Alminderej[1], Wael A. El-Sayed[2], Al Shimaa Gamal Shalaby[3], Sayed M. Saleh[1,4] and Tamer I. M. Ragab[3*]

[1]Department of Chemistry, College of Science, Qassim University, Buraidah 51452, Saudi Arabia
[2]Photochemistry Department, National Research Centre, Cairo 12622, Egypt
[3]Chemistry of Natural and Microbial Products Department, National Research Centre, Cairo 12622, Egypt
[4]Chemistry Branch, Department of Science and Mathematics, Faculty of Petroleum and Mining Engineering, Suez University, 43721 Suez, Egypt

(Received August 5, 2025; Revised April 17, 2026; Accepted September 17, 2026)

ABSTRACT. Date palm kernel (PK) is a valuable agricultural waste rich in phenolic compounds, sugars, carboxylic acids, and antioxidants, offering potential for medicinal applications. In this study, date palm kernel was extracted with 70% (v/v) ethanol–water, after which MCC and NCC were obtained from the residual biomass and fully characterized. Structural and morphological properties were analyzed using FTIR, EDXA, HRTEM, and SEM. Particle sizes ranged from 10–90 µm for MCC and 138–164 nm for NCC. The in-vitro cytotoxicity of the prepared cellulose was tested against MCF-7, HepG2, HCT-116, PC3, and A549 human cancer cell lines. Notably, NCC-PK showed significant cytotoxic activity against HCT-116 with an IC_{50} value of 40.56 ± 0.88 µg/mL. In addition, NCC-PK exhibited strong antibacterial activity, with a 20 mm inhibition zone against *Bacillus cereus*, *Bacillus subtilis*, and *Clostridium perfringens*. Prebiotic potential was also evaluated, where NCC-PK demonstrated a high prebiotic index (I=3.3) against *Lactobacillus casei*. The findings highlight the effective conversion of PK waste into bioactive cellulose materials with potential applications in biomedicine and functional food industries.

KEY WORDS: Date palm kernel, Nano-crystalline cellulose, Micro-crystalline cellulose, Anticancer, Prebiotic activity

INTRODUCTION

Utilizing natural resources and waste to achieve low-cost materials can increase industrial sustainability and reduce environmental pollution. Recently, green, renewable, and sustainable materials have gained considerable interest in providing different highly valued products possessing limited environmental influence [1-6].

Large quantities of date palm biomass waste are heaped up annually without suitable use. Date seeds, or kernels, are by–products (waste) of the date industry. Dates are a heavenly fruit cultivated in regions worldwide, including North Africa, the Middle East, and South Asia, especially in Al-Madinah, and are used for healing diseases. *Phoenix dactylifera*, or the date palm tree, belongs to the Arecaceae family, which contains 12–19 species of wild date palms. Dates also contain fiber and antioxidants and possess a high concentration of flavonoids and phenolic compounds, as well as a number of vitamins and minerals. Furthermore, dates have been proven to be beneficial for lowering the activity of amyloid beta proteins, which can form plaques in the brain, in several studies, including animal studies [7]. Eating dates may aid in reducing inflammation and avoiding the development of brain plaques, which may be crucial for preventing Alzheimer's disease. Palm kernel is used to treat wound healing, diabetes, eye disease, and reduce

*Corresponding authors. E-mail: tamerragab2006@gmail.com
This work is licensed under the Creative Commons Attribution 4.0 International License

skin wrinkles [8]. Palm kernel has found interest from a chemical point of view [9-12] and has shown biological impact, since PK coffee helps regulate blood sugar and is also used as animal feed. Date kernels are composed of carbohydrates, dietary fiber, fat, oil, ash, and protein. Palm kernel oil has amazing properties for wound healing and is used in cosmetic applications due to containing essential fatty acids, including linoleic, oleic, palmitic, and stearic acids. Date palm kernel extract exhibited antiviral effects against *Pseudomonas* phage ATCC 14209-B1 and prevented lysis of bacteria [13]. On the other hand, nanoparticle technology has reflected efficient improvement in drug delivery and led to promising properties such as size and increased efficiency. Targeted drug delivery using nanotechnology can open a new era in cancer therapy. Modern nanoparticles are developed to conjugate various cancer markers and penetrate inside the cancer cell due to cancer markers on its surface. The date palm fruit may contain chemo-preventive properties that protect against pancreatic cancer and possibly other cancers. The date palm fruit may be a good option for the development of commercial anticancer products based on natural compounds [14-16]. For the creation of commercial anticancer treatments based on natural chemicals, date palm fruit might be a promising choice. Considerable attention has been given to achieving efficient methods for the extraction of cellulose from palm [17-20]. In addition, the generation of nano- and microcrystalline cellulose, followed by investigation and confirmation, has attracted interest in this area [21-27], applying many spectral tools for structural confirmation [28-33].

The present study aimed to maximize the valorization of date palm kernel waste as a sustainable resource. Bioactive compounds were extracted using a 70% (v/v) ethanol–water solvent system to obtain a total extract rich in active constituents. Microcrystalline cellulose (MCC) and nanocrystalline cellulose (NCC) were subsequently isolated from the residual biomass and thoroughly characterized to evaluate their physicochemical properties.

Furthermore, the extracted bioactive compounds were separately loaded onto MCC and NCC matrices to develop functionalized biomaterials. These loaded systems were then evaluated for their in-vitro biological activities, including anticancer, prebiotic, antioxidant, and antibacterial effects. Overall, this study highlights the potential of date palm kernel waste as a renewable and cost-effective source for the production of high-value cellulose-based materials with promising applications in biomedical, pharmaceutical, and environmental fields.

EXPERIMENTAL

Palm kernel collection

PK was picked up from AL Tahhan Golden Dates Company at Siwa Oasis. After being collected, it was ground into powder using a grinding machine and dried in an oven set at 70 ºC until no more weight loss occurred.

Cell culture

The American Type Culture Collection (Rockville, Maryland, USA) sold three human cell lines: MCF-7 (human breast carcinoma cell line), Hep-G2 (liver carcinoma cell line), and HCT-116 (colon carcinoma cell line). The RPMI-1640 medium, 10% heat-inactivated FBS, 100 U/mL penicillin, and 100 U/mL streptomycin were used to sustain the cells. The cells were raised at 37° C in a humidified 5% CO_2 environment.

Culture media

Nutrient agar medium was used for cultivation and sustaining the pathogenic strains of Staphylococcus *aureus* and *E. coli*. MRS medium (Sharp, Rogosa, Medium). The latter was

prepared as a broth (without the inclusion) for ascertaining probiotic growth under investigation [34]. *L. Helveticus, L. reuteri,* and *L. casei* were developed and maintained in this medium. Base MRS medium contains the same inorganic components and nitrogen supply but at the same concentration, since it contains modified and extracted samples.

Microbial strains

Pathogenic organisms such as *E. coli*, *Bacillus cereus*, *Bacillus subtilis*, and *Clostridium perfrigenus* were isolated at the clinical laboratory (El Demerdash Hospital, Cairo, Egypt).

Phytochemical analysis

The collected PK composition wax, moisture, protein, ash, and low-molecular-weight carbohydrates (LMWC) were investigated. Carbohydrates of low molecular weight were determined by means of Soxhlet (85% ethanol solvent, 24 h, and then paper chromatography using aniline-phthalate spray). Quantitative investigation of monosaccharides was achieved by phenol-sulfuric acid, then color density measurement (480, 490 nm spectrophotometer UNICO 7200). Determination of the wax content was achieved by immersing the milled PF in toluene/EtOH (2:1) for 12 h, then filtering and extracting the oily residue (no active components of the milled PF (70% ethanol/water (10:1, v / w)) at 60 °C overnight.

Total phenolic content (TPC)

The extract (3 mL) was mixed with Folin-Ciocalteu phenol reagent (1.5 mL, 1:10 dilution in water), then left for 5 min. Na_2CO_3 (soln. 1.5 mL, 20%) was added, followed by stirring. Record the absorbance at 725 nm on a UV-1800 spectrophotometer after incubation (90 min, rt) (Shimadzu, Kyoto, Japan). Gallic acid was utilized for calibration of readings for the results to be expressed as mg.

Cellulose extraction

Extracted from dewaxed palm kernels (PK) was performed via NaOH (2.5%, 1–10 w/v) (3 h, 80 °C). The resulting crude cellulose then filtered out and dried (105 °C, three hours). The bleached form has been produced from its crude precursor applying NaClO (2–1 w/w) for two hours at 80 °C, followed by filtering. The product is obtained by neutralizing the cellulose residue with water and then drying it at 70 °C.

Preparation of MCC and NCC

α-Cellulose extraction has been achieved using the bleached form. Hydrolyzing the pure α-cellulose [2N sulfuric acid (1–10 w/v)] at reflux for nearly an hour afforded MCC, while NCC resulted from 2 N H_2SO_4 (1–15 w/v)via reflux for 90 min. Washing with water provides the MCC and NCC at neutral pH. By measuring the viscosity of cellulose samples (Guen solution) using a capillary viscometer of Ostwald submerged in a water bath at 25 °C, the viscosity of dissolved cellulose samples in cupriethylenediamine (Cuene) solution (the ratio between Cuene and PFC/RSC; P0.905 = 0.75 [η]/mL g^{-1}, where P is an unknown average DP) was investigated. The index of crystallinity (CI) was investigated applying Segal method

$$CrI\% = ((I_{002} - I_{am}))/I_{002}$$

I_{002}: the crystalline cellulose's intensity value, I_{am}: the amorphous cellulose's intensity value (2θ = 16°)

Formulation of extract-loaded nano- and microcrystalline cellulose

To prepare the active extract-loaded cellulose formulations, 100 mg of the palm kernel extract was mixed with 100 mg of either nanocrystalline cellulose (NCC) or microcrystalline cellulose (MCC). The mixture was dispersed in 0.5 mL of dimethyl sulfoxide (DMSO) and stirred at room temperature for 3 hours to ensure uniform adsorption of the active components onto the cellulose surface. The resulting formulations were then used for further biological evaluations.

Total carbohydrates estimation

A total of 0.5 mg of the sample was mixed with 0.5 mL of cold 80% sulfuric acid (H_2SO_4) and stirred until a paste was formed. The mixture was kept at room temperature for 15 hours to allow hydrolysis. Subsequently, more than 13 mL of distilled water was added to dilute the solution, which was then boiled in a sealed tube using a water bath for 6 hours. To neutralize the acidic solution, barium carbonate ($BaCO_3$) was added until effervescence ceased. The mixture was filtered, and the filtrate was passed through a column packed with Amberlite IR-120 [H^+] cation-exchange resin to remove excess ions. For colorimetric determination of total carbohydrates, 1 mL of 5% phenol solution was added to the sample, followed by the rapid addition of 5 mL concentrated H_2SO_4 with vigorous shaking. After 10 minutes at room temperature, the solution was allowed to stand at 20-30 °C for 20 minutes. The absorbance of the resulting colored complex was measured at 490 nm using a UNICO 7200 UV-visible spectrophotometer. The total carbohydrate content was quantified based on a standard calibration curve.

Qualitative examination and determination

The sugar extract was first treated with activated charcoal and boiled to remove impurities, followed by concentration under reduced pressure. The concentrated sugars were then subjected to paper chromatography using a solvent system composed of *n*-butanol/acetone/water (4:5:1, v/v/v). Reference monosaccharide standards were co-chromatographed for comparison. After development, the chromatograms were air-dried and sprayed with an aniline-phthalate reagent, prepared by dissolving phthalic acid (1.66 g) and aniline (48 mL) in a solvent mixture of *n*-butanol/diethyl ether/water (12:12:1, v/v/v). The chromatograms were then dried and heated at 105 °C for 10 minutes to visualize colored spots. The developed spots were excised, cut into small strips, and each was eluted with 4 mL of 0.7 N HCl in 80% ethanol. The absorbance of each eluate was measured at 390 nm for pentoses and 490 nm for hexoses using a UNICO 7200 UV-Vis spectrophotometer. Quantitative determination of monosaccharides was achieved by comparing absorbance values with standard calibration curves generated under identical conditions.

FT-IR spectroscopy

IR (Bruker Vectra 22 FT-IR) equipped with a Dura Sample IR II™ detector was applied for characterizing the afforded powder samples of biopolymers. The spectral resolution was set to 4 cm^{-1} over the wavenumber range 4000-400 cm^{-1}.

Scanning electron microscopy (SEM)

Scanning electron microscopy (JEOL 5410) was found to be a useful technique for examination of the surface morphology, conducted at 10 kV as an accelerating voltage. Samples of Cellulose

were gold-coated by means of a Hitachi coating unit (IB-2 coater, 0.1 Torr vacuum, 1.2 kV voltage, and 50 mA). For qualitative and quantitative analysis of elemental compositions, EDAX (or EDS) was applied.

Transmission electron microscopy (TEM)

MCC and NCC morphology and size were recorded by means of TEM (JEOL-JEM1011, Japan). Minor drops of nanoparticle suspension were placed on a carbon-coated copper grid, and then evaporation of the solvent allowed the TEM image to be recorded.

GC-MS analysis

To analyze the active components in the palm kernel (PK) extract, silylation was performed prior to GC-MS analysis. Briefly, 100 mg of PK extract was dissolved in 5 mL of 70% ethanol, followed by sonication for 30 minutes. The solution was then centrifuged at 12,000 rpm for 10 minutes. An aliquot of 100 µL of the supernatant was transferred to screw-cap vials and evaporated to dryness under a stream of nitrogen gas. The dried residue was derivatized by adding 150 µL of N-methyl-N-(trimethylsilyl)trifluoroacetamide (MSTFA) mixed with anhydrous pyridine (1:1, v/v), and incubated at 60 °C for 45 minutes. The resulting silylated derivatives were diluted (1:10, v/v) with hexane, and 1 µL was injected into the GC–MS system. Chromatographic separation was carried out using an Rtx-5MS capillary column (30 m × 0.25 mm i.d., 0.25 µm film thickness). Electron impact (EI) ionization was performed at 70 eV, and mass spectra were recorded in the 40-450 m/z range.

Compound identification was conducted using Automated Mass Spectral Deconvolution and Identification System (AMDIS) software, comparing the obtained spectra to those in the Wiley and NIST spectral libraries. Retention indices (RI) were calculated based on a homologous series of n-alkanes (C6-C20) for further confirmation of compound identity.

Antibacterial activity

The antibacterial activity of the extracted and modified materials was evaluated using the well diffusion method as described by [35]. The assay was performed against *Bacillus cereus*, *Bacillus subtilis*, and *Clostridium perfringens*. Briefly, 20 mL of sterile nutrient agar was poured into Petri dishes and allowed to solidify. After solidification, each plate was seeded with bacterial cultures adjusted to approximately 10^6 CFU/mL using sterile saline solution. The inoculum (150 µL) was evenly spread across the agar surface using a sterile glass spreader. Wells (4 mm diameter) were then punched into the agar using a sterile cork borer. Each test sample was prepared at a concentration of 150 µg/mL, diluted in 1 mL of distilled water, sterilized by filtration through a 0.22 µm membrane filter, and subsequently added (100 µL) into the respective wells. The plates were incubated at 37 °C for 24 hours, and the zones of inhibition were measured in millimeters to assess antibacterial activity.

Prebiotic activity

The prebiotic potential of the extracted and modified materials was evaluated through their ability to support the growth of probiotic strains, following methods described in previous studies [36, 37]. *Escherichia coli* was cultivated on nutrient medium as a reference strain, while the probiotic strains *Lactobacillus casei*, *Lactobacillus reuteri*, and *Lactobacillus helveticus* were cultured in de Man, Rogosa and Sharpe (MRS) medium. All strains were incubated at 37 °C for 24 hours. For the assay, 10 mL of each culture medium was supplemented with 150 mg of the test material. Aliquots (0.1 mL) of actively growing cultures were used as inoculum. Following incubation

(37 °C, 24 h), bacterial growth was monitored by measuring the optical density (OD) at 625 nm using a spectrophotometer. A sterile, uninoculated medium served as the blank control. The prebiotic activity of the materials was quantified using the Prebiotic Index (PI), calculated based on the differential growth promotion of probiotics relative to the control strain (*E. coli*).

Antioxidant activity (DPPH assay)

The free radical scavenging capacity of the extracted and modified samples was evaluated using the 2,2-diphenyl-1-picrylhydrazyl (DPPH) assay, following the procedure described by Hwang and Thi [38], with slight modifications. Stock solutions of the test samples were prepared by dissolving 10 mg of each material in 1 mL of dimethyl sulfoxide (DMSO), and serial dilutions were made to obtain different concentrations. For each concentration, 10 µL of the sample solution was mixed with 90 µL of freshly prepared DPPH solution (in methanol) in the wells of a 96-well ELISA microplate. The mixtures were incubated in the dark for 35 minutes at room temperature to prevent photodegradation of DPPH. Absorbance was measured at 517 nm using a microplate reader (ELISA reader). The percentage of DPPH radical scavenging activity was calculated using the following equation:

Scavenging activity (%) = $(A_0 - A_s/A_0) \times 100$

Where:
A_0 = absorbance of the control (DPPH + DMSO)
A_s = absorbance of the sample (DPPH + test material)

Cytotoxicity activity

MTT method was used to measure the vitality of the cells for investigating the cytotoxicity influence. The operations were completed in a bio-safety sterile class(II) Laminar Flow Cabinet (Baker, SG403INT, Sanford, ME, USA). The media (RPMI 1640: HePG2, MCF7 and HCT116) or (DMEM: A549 and PC3), antibiotic-antimitotic mixture (1%, K-Penicillin (10,000U/mL), Streptomycin-SO_4 (10,000g/mL), and Amphotericin B (25g/mL)), and L-glutamine (1%) were used to suspend the cells. The temperature was left at 35-37°C with CO_2(5%). Using a water-jacketed incubator (CO_2), cells were batch grown for 10 days before being seeded in 96-well microtiter plastic plates at a concentration of 10x103 cells/well in fresh growth media (Sheldon, TC2323, Cornelius, OR, USA).
Incubation was performed either as a negative control or with varied concentrations of samples (100, 50, 25, 12.5, 6.25, 3.125, 0.78, and 1.56 ug/mL). Aspiration, then fresh media addition followed by incubation, was performed. Aspirated medium (40 µL) (incubated for 48 hours) was provided with MTT salt (2.5 µg/mL), then further incubated for four hours at 37 ºC with 5% CO_2. Sodium dodecyl sulfate (SDS) (200 µL, 10%) in deionized H2Owas added, then incubated overnight at (37 ºC) using a positive control [39, 40]. The values were recorded at 595 nm (620 nm, ref. wavelength). The statistical significance between the samples and the negative controls (cells containing a vehicle) was investigated using the SPSS 11 software and an independent t-test. The chosen solvent was DMSO, which was found suitable for the extract, at a concentration of less than 0.2%. The formula used to determine the viability change % was as follows:

(Observed value of extract/control) -1) x 100

Using the SPSS 11 program, a probit analysis was performed to determine the IC_{50} and IC_{90} values. The National Research Center, El-Tahrir St., Dokki, Cairo 12622, Egypt, conducted the cytotoxic activity test (*In vitro* bioassay on human tumor cell lines).

Statistical analysis

A repeated-measures ANOVA was used, followed by the least significant test for multiple comparisons. At $p < 0.05$, the effects are deemed significant. Results are given as the mean ± standard error. The Kruskal-Wallis non-parametric one-way ANOVA was used to statistically analyze the stomach ulcer scores, followed by the Mann-Whitney test. $p < 0.05$ revealed a significant difference from the ethanol control group.

RESULTS AND DISCUSSION

Chemical composition and total carbohydrates

The chemical composition of palm kernel (PK) was thoroughly examined, focusing on its content of moisture, ash, wax, low-molecular weight carbohydrates (LMWC), and protein. The results showed the following percentages (w/w): moisture 2.5%, wax 1.6%, ash 2.2%, LMWC 3.6%, and protein 1.8%. A more detailed analysis revealed additional constituents, including moisture (3.19%), ash (1.21%), protein (12.20%), lipids (7.97%), flavonoids (1615.12 mg/100 g), tannins (139 mg/100 g), total phenolics (1834.22 mg/100 g), and dietary fiber (64.3%). Comparative values for rice husk and rice straw were also recorded. For rice husk, the contents of LMWC, lipids, wax, ash, and moisture were 7.35%, 2.15%, 5.85%, 17.65%, and 12.41%, respectively, whereas rice straw presented corresponding values of 4.20%, 5.45%, 12.55%, 14.20%, and 9.20%.

To assess the total carbohydrate content and crude cellulose in PK, acid hydrolysis followed by separation and paper chromatography was employed. The total carbohydrate yield from PK was 20.6%; however, this relatively low yield may be attributed to losses during the dewaxing process. These results align with prior studies on roasted date pits, which reported sugar contents between 11.1–15.0%. In contrast, rice husk and rice straw demonstrated significantly higher sugar levels at 64.6% and 62.4%, respectively [41]. Qualitative and quantitative sugar profiling of PK identified the presence of key monosaccharides in the following proportions: D-galacturonic acid (5%), D-galactose (15%), L-arabinose (50%), and D-mannose (30%). In terms of antioxidant potential, the high total phenolic content of PK (844.81 mg/100 g) is particularly noteworthy. Seventeen distinct phenolic compounds were identified in PK, including cinnamic acid, pyrogallol, ellagic acid, benzoic acid, protocatechuic acid, catechol, caffeine, syringic acid, vanillic acid, chlorogenic acid, epicatechins, p-hydroxybenzoic acid, ferulic acid, catechin, gallic acid, caffeic acid, and 4-aminobenzoic acid. The abundance of these bioactive compounds suggests that PK may serve as a valuable raw material for pharmaceutical and nutraceutical applications, highlighting its industrial potential beyond traditional uses.

GC–MS analysis of silylated PK extract

According to the data summarized in Table 1, a total of 31 major components were identified, representing 99.34% of the total PK extract. The composition was dominated by carbohydrates, followed by phenolic compounds, carboxylic acids, and several minor constituents. Among the identified carbohydrates, sucrose was the most abundant, accounting for 49.52%, followed by D-[+]-mannopyranose (13.99%), D-[-]-fructopyranose (6.94%), raffinose (3.91%), and oleanitrile (3.16%) (Figure 1). One of the key acidic sugars identified was D-galacturonic acid, a vital uronic acid that plays a significant role in various metabolic pathways within the human body. Notably, arabinose, which is known to inhibit the enzymatic hydrolysis of sucrose in the small intestine, was also detected. In this pathway, sucrose is broken down into glucose and fructose. Due to its ability to interfere with sucrose absorption, arabinose-containing foods and beverages are frequently developed for diabetic and prediabetic populations. Additionally, arabinose shows

promise as a prebiotic, since it is not absorbed in the intestine and serves as a carbon source for beneficial gut microbiota such as Bifidobacteria [42]. Mannose, another major sugar detected, is recognized for its involvement in the glycosylation of specific proteins critical to human cellular metabolism and immune function [43].

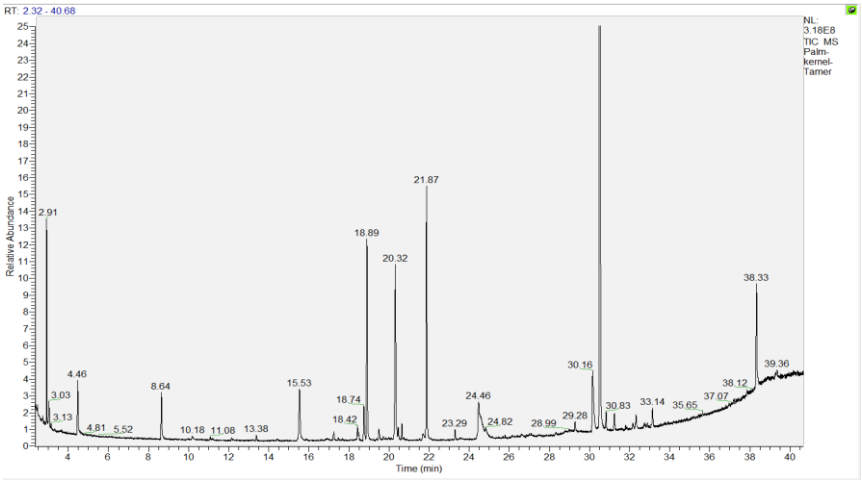

Figure 1. The chromatograms of the composition of palm kernel extract 70% ethanol

Table 1. The composition and percentage composition of palm kernel extract 70% ethanol, n= 3).

No.	RT	Area %	Name
1	2.91	3.68	Ethylamin
2	3.03	0.69	2,6,8-Trimethyl-1,2-Dihydroquinoline
3	4.46	1.73	D-Lactic acid-DITMS
4	8.64	1.58	3,7-Dioxa-2,8-disilanonane, 2,2,8,8-tetramethyl
5	15.53	2.21	2-Piperidinecarboxylic acid
6	17.23	0.29	Ribitol
7	18.42	0.41	D-[-]-Tagatofuranose
8	18.74	1.33	D-Psicofuranose
9	18.89	6.94	D-[-]-Fructopyranose
10	20.31	6.53	D-[+]-Mannopyranose
11	20.46	0.26	D-[+]-Talopyranose
12	20.64	0.63	Mannitol TMS
13	21.68	0.33	Hexadecanenitrile
14	21.87	7.46	D-[+]-Mannopyranose
15	23.29	0.33	Myo-Inositol
16	24.46	3.16	Oleanitrile
17	24.83	0.28	Hexadecanenitrile
18	30.16	2.94	D-[+]-Turanose
19	30.52	49.52	Sucrose TMS
20	30.83	0.62	Monopalmitin2TMS
21	31.24	0.62	4-O-á-Galactopyranosyl-D-mannopyranose
22	32.16	0.31	2-à-Mannobiose
23	32.32	0.50	4-O-á-Galactopyranosyl-D-mannopyranose
24	32.74	0.25	D-[+]-Cellobiose
25	32.88	0.24	1-Monooleoylglycerol

26	33.14	0.70	Pentaisopropyl 5TMS
27	34.05	1.00	Palmiticacid
28	35.65	0.32	D-Glucopyranosiduronic acid
29	37.19	0.28	Ethyl iso-allocholate
30	38.33	3.91	RaffinoseTMS
31	39.94	0.29	9-Octadecenoic acid

Crude cellulose extraction and estimation

Crude cellulose was successfully extracted from palm kernel (PK) agricultural residue with a notable yield, highlighting the potential of PK as a renewable biomass source. Among the examined materials, palm fronds (PF) demonstrated the highest crude cellulose content, reaching 60.02% (w/w). The optimization of the alkaline extraction process was effective, as it employed a relatively low concentration of 2.5% NaOH for 3 hours at 80 °C, leading to enhanced cellulose recovery. Comparative analysis of date palm fibers and fronds revealed cellulose contents of 40.21% and 38.26%, hemicellulose contents of 12.80% and 28.17%, and lignin levels of 32.21% and 22.52%, respectively. The alkaline treatment caused cellulose swelling and partial dissolution of lignin and silica, which resulted in a decrease in cellulose crystallinity. Due to the intricate network in plant cell walls, where hemicelluloses are covalently and hydrogen-bonded to cellulose and lignin, their separation remains challenging without structural disruption. The recovered raw cellulose showed a carbohydrate content of 65.20%. Based on paper chromatography analysis, the sugar composition included D-glucose (62%), D-xylose (22%), L-arabinose (11%), and glucuronic acid (5%). Although purified cellulose ideally consists of repeating units of D-glucose only, the presence of hemicellulose-derived sugars suggests incomplete separation during extraction. However, the bleaching and alkaline hydrolysis procedures proved effective, as evidenced by a bleached cellulose yield of 99% and a degree of polymerization (DP) of 520 for the crude cellulose. These results confirm the efficiency of the extraction protocol in removing both hemicellulose and lignin, thereby enhancing the structural integrity and purity of the cellulose fraction.

Preparation and characterization of MCC and NCC

Crude cellulose was efficiently extracted from palm kernel (PK) agricultural residue, underscoring its potential as a valuable renewable biomass source. Among the studied biomaterials, palm fronds (PF) exhibited the highest cellulose content, reaching 60.02% (w/w). The alkaline extraction process was optimized using 2.5% NaOH for 3 hours at 80 °C, resulting in improved cellulose recovery. A comparative compositional analysis of date palm fibers and fronds revealed respective cellulose contents of 40.21% and 38.26%, hemicellulose contents of 12.80% and 28.17%, and lignin levels of 32.21% and 22.52%. Alkaline treatment facilitated the swelling of cellulose fibers and partial dissolution of lignin and silica, thereby reducing cellulose crystallinity. However, the tight association between hemicelluloses, lignin, and cellulose mediated by covalent and hydrogen bonding complicates their complete separation without structural alteration. The extracted raw cellulose contained 65.20% carbohydrates. Paper chromatography analysis identified the major monosaccharide constituents as D-glucose (62%), D-xylose (22%), L-arabinose (11%), and glucuronic acid (5%). Although pure cellulose is composed exclusively of D-glucose units, the presence of additional sugars indicates residual hemicellulose fractions. Nevertheless, the integrated bleaching and alkaline hydrolysis steps proved highly effective, yielding 99% purified cellulose with a degree of polymerization (DP) of 520. These results confirm the efficiency of the extraction protocol in removing lignin and hemicellulose, while preserving the structural integrity and high purity of the cellulose.

FT-IR analysis

FT-IR is a key tool for the investigation of functional groups. Following alkaline extraction, there were typically some spectral changes shown by variations in band intensity and vanishing (Figure 2A). The three forms involving α-cellulose, bleached, and Crude displayed distinctive patterns capable of comparison. The bands (*str.*) related to OH groups have been shown between 3310 and 3420 cm^{-1}. The absorption band at 1555 cm^{-1} was assigned to the nonsymmetric C–O–C bridge, while the value at 2905-2850 cm^{-1} was associated with the stretched C–H absorbance of the cellulose -CH_2. Since cellulose and water interact greatly, particularly when cellulose is raw or bleached, the observed absorption at 1632 cm^{-1} was ascribed to the absorption of water molecules. The band at 1410- 440 cm^{-1} was associated with polysaccharide C- H in addition to OH and CH2 vibrations (bending). Additionally, the revealed absorptions around 1040–1095 were linked to the C–O–C stretching vibrations or ring stretching of the polysaccharide. C- C stretching, ether bond, or C-O-H in hemicelluloses was revealed at 1035 cm^{-1} in crude cellulose spectra. Previous studies claim that all lignin has been entirely eliminated from α-cellulose since there are no peaks in the range between 1505 and 1560, that is related to bi-bonding vibrations in aromatic. 880 cm^{-1} absorption suggested for the β-linkage nature connecting glucose units. The band at 894-897 cm^{-1} is associated with the anomeric vibration of *β*-glucosides (C-H rock vibration of cellulose). The bands between 2850 and 2910 cm^{-1} are assumed to result from the cellulose's crystalline structure (Figure 2B).

It was demonstrated that alkaline treatment can provide crystalline cellulose (type I structure). The variation of the NCC and MCC crystalline index revealed a sharper peak intensity and an enhanced crystallinity degree compared to the crude form. The peaks at 1365-1375 are connected to the asymmetric C-H disfigurement. These peaks match the ideal identity of pure MCC [43]. The single OH bond (*str.*) was identified as the cause of the large absorbance band seen in the MCC and NCC spectra in the 3400-3550 cm^{-1} range.

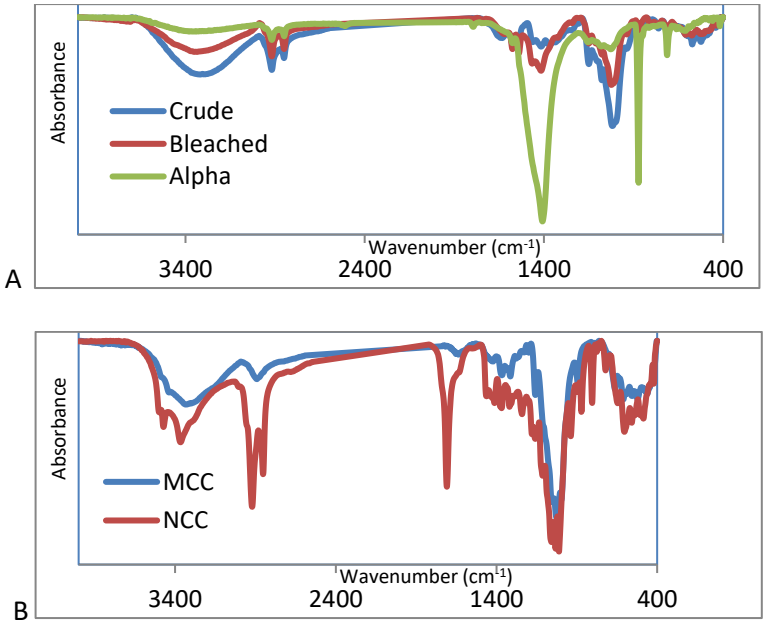

Figure 2. FT-IR spectra of (A) crude, bleached, α-cellulose palm kernel and (B) MCC, NCC palm kernel.

SEM analysis

Scanning Electron Microscopy (SEM) was employed to examine the morphological structure of various cellulose samples derived from palm kernel (PK). The SEM micrographs revealed significant structural transformations at each processing stage, highlighting the progressive purification of cellulose. As illustrated in Figure 3, SEM images taken at a magnification scale of 50 μm displayed noticeable differences in surface morphology among PK, crude cellulose, bleached cellulose, α-cellulose, microcrystalline cellulose (MCC), and nanocrystalline cellulose (NCC). The raw PK fibers exhibited heterogeneous, irregular surfaces with embedded cellular structures, indicative of the presence of cellulose interspersed with hemicellulose, lignin, and other plant components. Crude cellulose maintained a fibrous structure but showed the persistence of hemicellulose and lignin residues, as evidenced by the irregular surface features. Bleached cellulose showed improved structural uniformity, though traces of lignin and hemicelluloses were still visible. In contrast, α-cellulose exhibited a more purified, continuous fibrous morphology, indicating effective removal of non-cellulosic materials. MCC demonstrated well-defined, crystalline fibers in the 12–95 μm range, characterized by compact and individualized fiber bundles. NCC, on the other hand, displayed a nano-scaled fibrous network within the 210–410 nm range. Although NCC fibers appeared less crystalline than MCC, they showed uniform dispersion and consistent morphology, indicative of successful nano-structuring. These observations confirm the progressive purification and structural refinement of cellulose during the extraction and modification processes.

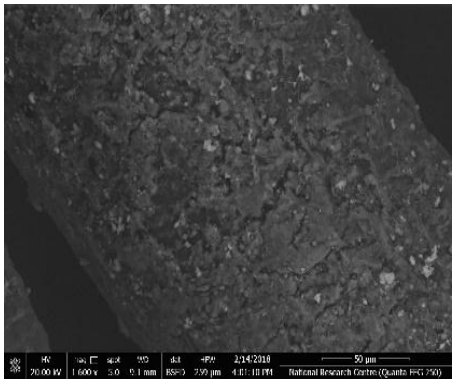

PK

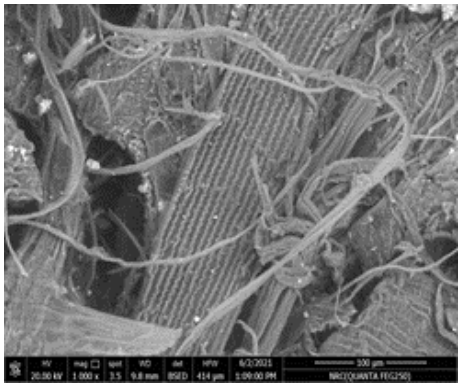

Crude cellulose

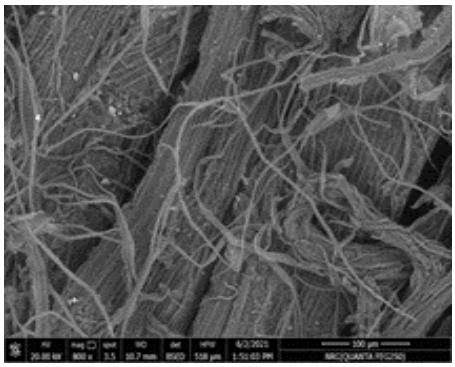

Bleached

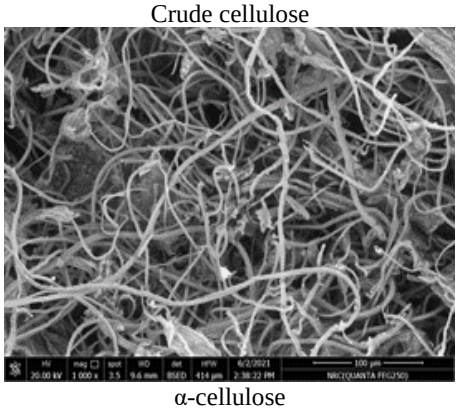

α-cellulose

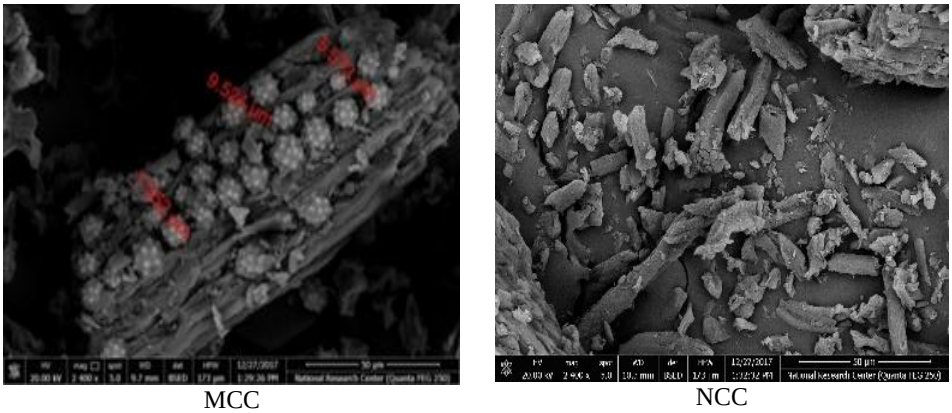

MCC NCC

Figure 3. SEM images and histograms of the PK, crude cellulose PK, bleached cellulose PK, α-cellulose PK, MCC and NCC PK samples.

TEM analysis

High-Resolution Transmission Electron Microscopy (HRTEM) was utilized to investigate the morphology and particle size distribution of microcrystalline cellulose (MCC) and nanocrystalline cellulose (NCC) (Figure 4). The analysis revealed that both MCC and NCC particles exhibited predominantly spherical or near-spherical shapes. MCC particles displayed a broader size range, spanning from 10 to 90 µm, indicative of their micro-scale structure and crystalline integrity. In contrast, NCC particles showed significantly smaller dimensions, ranging from 138 to 164 nm, confirming their nanoscale nature. The observation that all NCC particles were below 164 nm highlights their potential for enhanced biological activity and surface reactivity, particularly in applications such as drug delivery, antimicrobial systems, and biodegradable composites. Moreover, the clear spatial separation between particles in the NCC samples suggests that bioactive compounds present in the plant extract may have contributed to a capping or stabilizing effect during synthesis. This phenomenon likely prevented particle agglomeration, thereby maintaining uniform nanoscale dispersion.

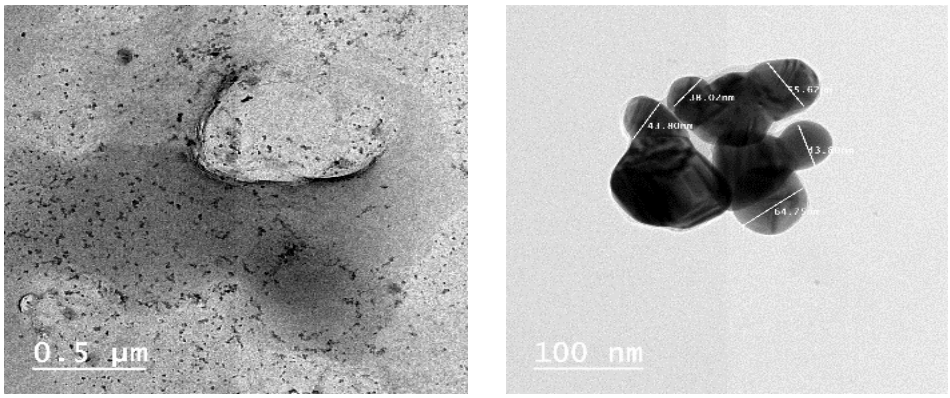

MCC NCC

Figure 4. TEM images of MCC and NCC palm kernel.

EDAX analysis

Energy-Dispersive X-ray Analysis (EDAX), a cutting-edge technique for micro- and nano-scale elemental characterization, was employed to identify the elemental composition of MCC and NCC samples (Figure 5). The results indicated the presence of several elements, including carbon (C), nitrogen (N), oxygen (O), sodium (Na), magnesium (Mg), aluminum (Al), silicon (Si), sulfur (S), calcium (Ca), potassium (K), manganese (Mn), iron (Fe), and nickel (Ni) in varying proportions. In NCC, a noticeable reduction in the concentration of several elements was observed compared to MCC. This reduction is likely attributed to the intensive acid hydrolysis treatment during NCC preparation, which may have removed or leached out non-cellulosic components and mineral residues. Despite the reduced elemental ratios, these elements—especially trace metals like Fe, Mg, and Mn may contribute to the functional activation and potential bioactivity of MCC and NCC, enhancing their value for biomedical and pharmaceutical applications.

In comparison, EDAX analysis of raw palm kernel (PK) samples revealed a broader elemental profile, comprising C, O, N, Na, Mg, P, Cl, K, Ca, and Fe. This rich elemental diversity underscores PK's potential as a nutritionally valuable biomass, with elements that are known to participate in various human metabolic and physiological processes. These findings not only confirm the structural transformation of cellulose during processing but also highlight the biological relevance of the remaining mineral content in MCC and NCC, which may play a role in their functional performance in diverse applications.

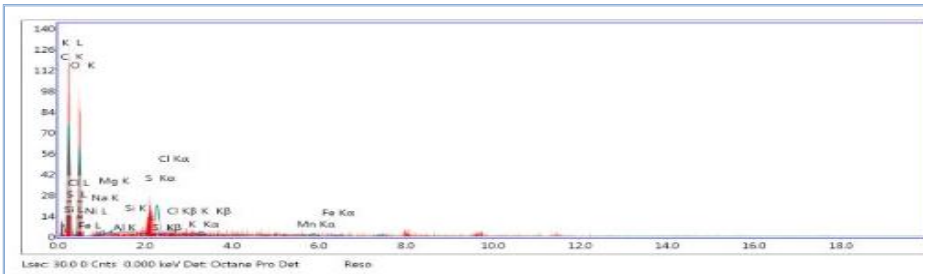

Element	Weight %	Atomic %	Net Int.	Error %
C K	50.32	59.4	36.99	10.3
N K	1.42	1.43	0.27	99.99
O K	40.91	36.26	29.82	13.64
NaK	0.62	0.38	1.2	73.34
MgK	0.21	0.12	0.76	76.97
AlK	0.22	0.12	1	73.12
SiK	0.24	0.12	1.29	69.61
S K	2.68	1.19	13.64	14.14
ClK	0.57	0.23	2.59	62.96
K K	0.42	0.15	1.64	65.51
MnK	0.73	0.19	1.27	67.27
FeK	0.63	0.16	0.96	69.74
NiK	1.02	0.25	1.16	68.22

MCC

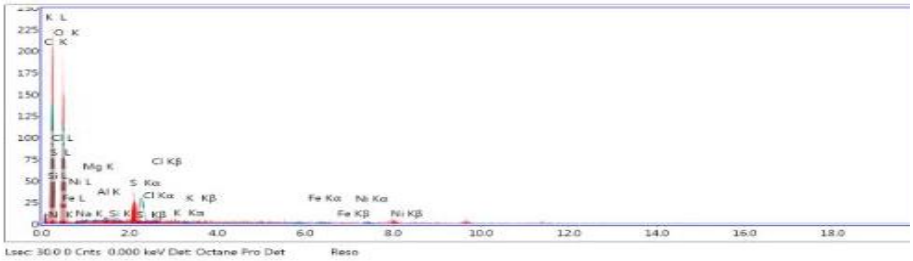

Element	Weight %	Atomic %	Net Int.	Error %
C K	50.05	58.8	68.14	9.14
N K	0.73	0.74	0.25	99.99
O K	43.01	37.93	57.69	11.96
NaK	0.61	0.37	2.06	69.9
MgK	0.24	0.14	1.52	70.36
AlK	0.38	0.2	3.08	64.69
SiK	0.3	0.15	2.82	63.82
S K	2.21	0.97	19.88	11.45
ClK	0.39	0.16	3.16	61.61
K K	0.21	0.08	1.47	65.93
MnK	0.51	0.13	1.55	65.6
FeK	0.54	0.14	1.47	66.09
NiK	0.83	0.2	1.67	65.21

NCC

Figure 5. Energy dispersive X-ray analysis (EDXA) of MCC and NCC palm kernel.

Antibacterial activity

The antibacterial efficacy of the extracted compounds was evaluated by measuring the diameter of the inhibition zones against selected pathogenic bacteria. All tested samples exhibited varying degrees of antibacterial activity, with notable inhibition observed particularly against *Bacillus cereus*, *Bacillus subtilis*, and *Clostridium perfringens*. As shown in Table 2, the inhibition zones reached up to 20 mm in diameter for these bacterial strains. Both microcrystalline cellulose (MCC) and nanocrystalline cellulose (NCC) demonstrated enhanced antibacterial activity compared to the control and other tested samples. The superior performance of the nano- and micro-scale celluloses may be attributed to their increased surface area, improved dispersibility, and potential for interaction with bacterial membranes, thereby disrupting cellular functions. These findings suggest that the extracted cellulose derivatives, particularly in nano- and microforms, possess promising antibacterial properties, making them potential candidates for applications in biomedical materials, food packaging, and antimicrobial formulations.

Prebiotic activity

The objective of prebiotic activity is to stimulate the growth of beneficial gut microbiota. In this study, the prebiotic potential of palm kernel (PK), nanocrystalline cellulose derived from PK (NCCPK), and microcrystalline cellulose derived from PK (MCCPK) was assessed by evaluating their ability to promote the growth of probiotic strains and inhibit the proliferation of pathogenic bacteria. The experimental design involved culturing *Lactobacillus reuteri* and *Lactobacillus*

casei (probiotic strains), as well as *Escherichia coli* (a common intestinal pathogen), in MRS media supplemented with PK, MCCPK, or NCCPK as the sole carbohydrate source. Growth densities were measured, and prebiotic activity indices were calculated by comparing the optical density (OD) of probiotic versus pathogenic growth. As presented in Table 2, all tested samples exhibited prebiotic activity, with enhanced growth of *L. casei* and *L. reuteri* relative to *E. coli*. The highest prebiotic activity index (I = 3.3) was recorded for NCCPK with *L. casei*, indicating strong selectivity in promoting probiotic over pathogenic growth. Conversely, the lowest index (I = 1.6) was observed for MCCPK with *L. reuteri*, though still indicative of a positive prebiotic effect. These results support the potential of PK-derived celluloses, especially in their nanoform, as functional food ingredients with selective prebiotic properties.

Table 2. Antibacterial activity and prebiotic activity.

Compound	Diameter zone			Prebiotic index	
	Bacillus cereus	*Bacillus subtilis*	*Clostridium perfrigenus*	*L. casei*	*L. reuter*
PK	17 ± 0.2	17 ± 0.1	18 ± 0.2	3.2	3.17
NCCPK	20 ± 0.3	20 ± 0.2	20 ± 0.3	3.3	2.7
MCCPK	19 ± 0.1	17 ± 0.3	17 ± 0.1	2.5	1.6
Control	20 ± 0.2	20 ± 0.1	20 ± 0.2	-----	-----

Antioxidant activity

The antioxidant potential of palm kernel (PK), microcrystalline cellulose (MCCPK), and nanocrystalline cellulose (NCCPK) was assessed using the DPPH radical scavenging assay. The results revealed high antioxidant activities, measured at 80% for PK, 82% for MCCPK, and 83% for NCCPK, respectively. The slight enhancement in activity observed with MCCPK and NCCPK is likely attributed to improved surface area and delivery properties associated with the micro- and nano-structured forms of cellulose. A strong correlation between total phenolic content and antioxidant activity was noted, supporting previous findings. For instance, [46] reported that date seed kernel extract exhibited approximately 81% antioxidant activity, aligning well with the current findings. Additionally, another study [47] evaluated antioxidant capacities of date kernels from various cultivars, with reported values ranging between 78.03 mg/mL (Monaif) and 79.94 mg/mL (Barhi cv.), further validating the high radical-scavenging potential of kernel-based materials. These findings highlight the promise of PK-derived materials especially in their modified forms as natural antioxidant agents for potential application in nutraceuticals and functional foods.

Cytotoxic activity

The in vitro cytotoxic potential of palm kernel extract (PK), microcrystalline cellulose from PK (MCC PK), and nanocrystalline cellulose from PK (NCC PK) was investigated using the MTT assay against five human cancer cell lines: MCF-7 (breast), HEPG-2 (liver), HCT-116 (colon), PC3 (prostate), and A549 (lung). The IC_{50} values for each sample were determined and are presented in Figure 6. Among the tested samples, NCC PK exhibited the most potent cytotoxic activity, particularly against the HCT-116 colon cancer cell line, with an IC_{50} value of 40.56 ± 0.88 µg/mL. This enhanced cytotoxicity is attributed to improved drug delivery and cellular uptake, likely due to the nano-scale particle size and surface interaction of the NCC matrix. The cytotoxic performance followed the order: HCT-116 > HEPG-2 > MCF-7, indicating that colon and liver cancer cells were more susceptible to treatment with the tested samples, while MCF-7 (breast cancer cells) demonstrated the least sensitivity. Against A549 (lung) and PC3 (prostate) cell lines, NCC PK and MCC PK showed moderate to low activity, with IC_{50} values ranging from 24.30 to 52.66 µg/mL. Overall, NCC PK demonstrated the highest bioactivity, followed by MCC

PK, while the unmodified PK extract showed the weakest cytotoxic effect across all five cancer cell lines, as illustrated in Figure 7. Analytical results confirmed that the extracted microcrystalline cellulose (MCC) and nanocrystalline cellulose (NCC) were devoid of heavy metals typically implicated in cytotoxic responses [48, 49]. The data suggest that nanostructuring significantly enhances the therapeutic potential of PK-derived materials, particularly against colorectal and hepatic cancers.

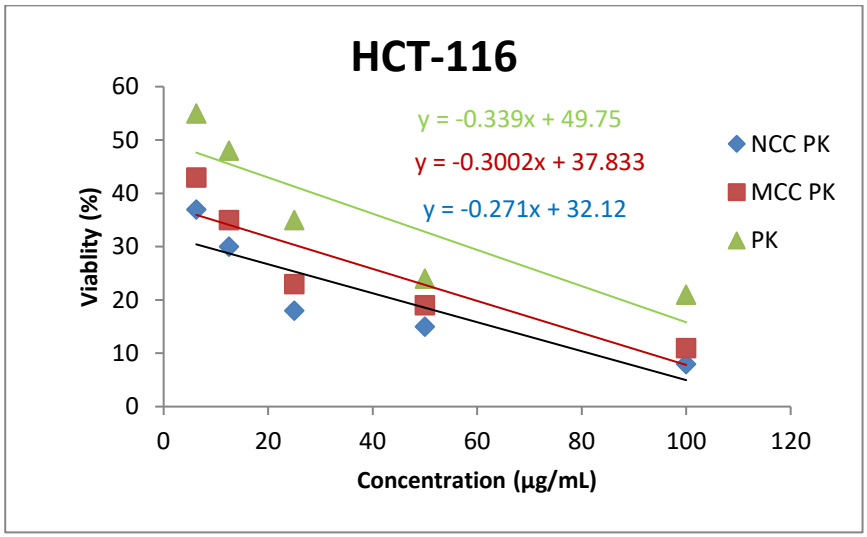

a

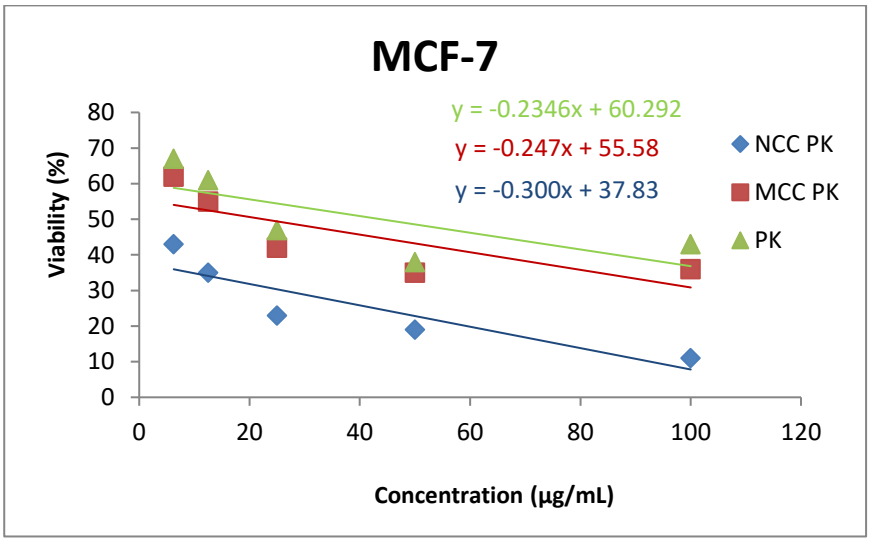

b

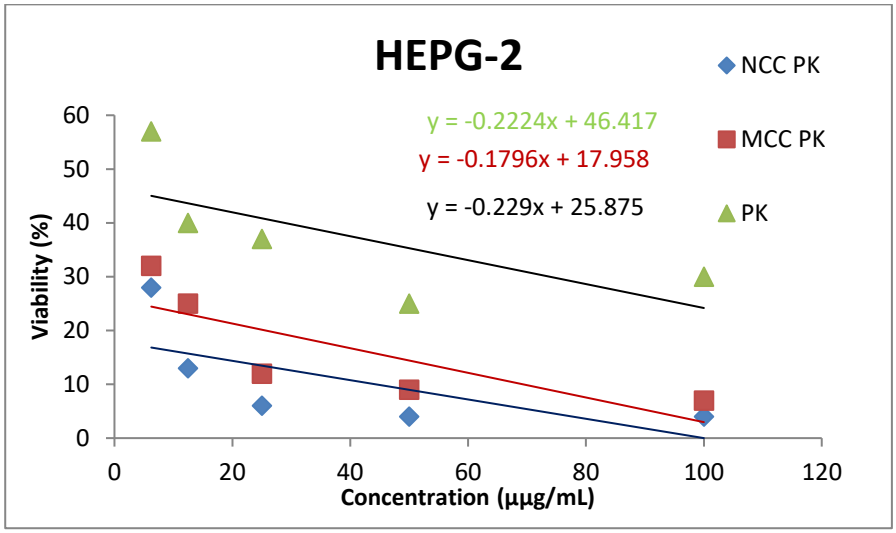
HEPG-2
NCC PK
MCC PK
PK
y = -0.2224x + 46.417
y = -0.1796x + 17.958
y = -0.229x + 25.875
Viability (%)
Concentration (µµg/mL)
0
10
20
30
40
50
60
0
20
40
60
80
100
120

c

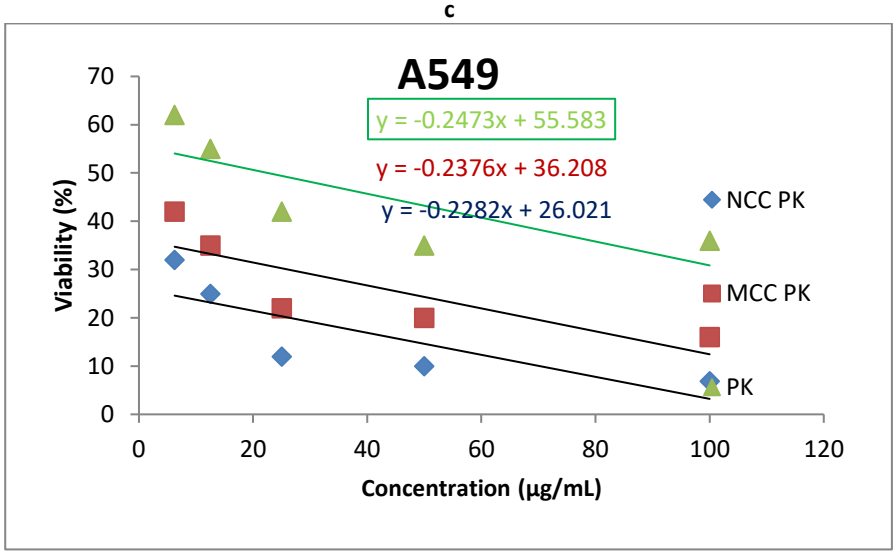
A549
y = -0.2473x + 55.583
y = -0.2376x + 36.208
y = -0.2282x + 26.021
NCC PK
MCC PK
PK
Viability (%)
Concentration (µg/mL)
0
10
20
30
40
50
60
70
0
20
40
60
80
100
120

d

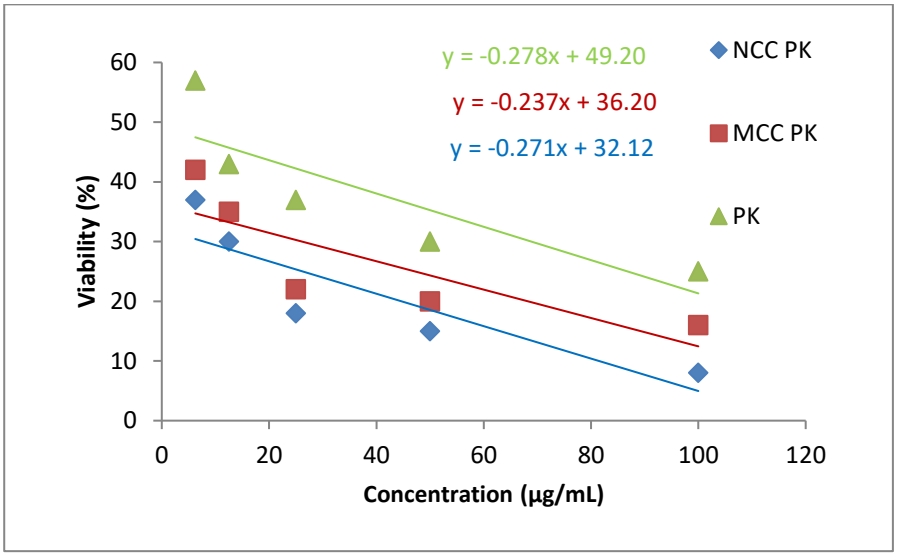

e

Figure 6. PK, MCC PK and NCC PK effect on the viability of cell line (a) HCT-116 (b) HEPG-2 (c) MCF-7, (d) PC3and (e) A549.

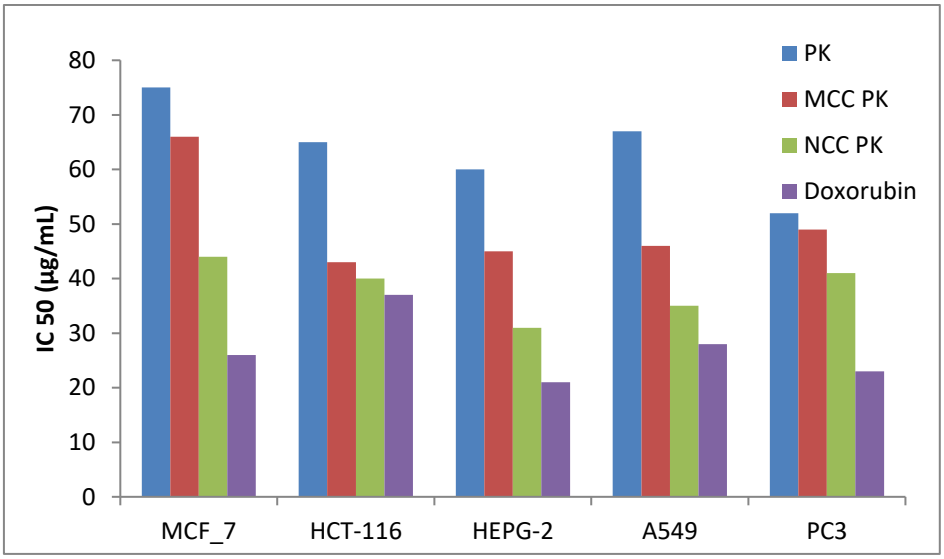

Figure 7. The IC_{50} values of PK, MCC PK, and NCC PK.

IC_{50}: Lethal concentration of the sample that causes the death of 50% of cells in 48 hrs.
Positive control: Adriamycin (Doxorubicin)(Mw= 579.99).

CONCLUSION

Nano-crystalline cellulose (NCC) and micro-crystalline cellulose (MCC) were efficiently prepared from palm kernel extract and well characterized. The prepared PKNCC and PKMCC have revealed improved biological effects compared to their corresponding PK samples. The prepared PKNCC showed good anticancer activity against a number of human cancer cell lines; the most susceptible were the HCT-116 and HEPG-2 cancer cell lines, in addition to good antibacterial and antioxidant properties. Developing nanoparticles of nano- and microcrystalline cellulose carriers that contain palm kernel extract enhances properties by helping to reach the desired site of action, subsequently improving prebiotic, anticancer, and antibacterial activities. The results reveal the importance of nanoparticle technology which has the ability to promote research into novel and modified PKNCC for developing novel anticancer agents. The study demonstrates that nano- and microcrystalline cellulose derived from palm kernel significantly enhance the biological activities of the extract, including anticancer, antibacterial, antioxidant, and prebiotic effects, highlighting the potential of these cellulose-based nano-carriers for targeted delivery applications, while suggesting that further optimization and in vivo studies are needed to advance their translational potential in developing novel therapeutic agents.

ACKNOWLEDGMENT

This article is derived from a research grant funded by the Research, Development, and Innovation Authority (RDIA) - Kingdom of Saudi Arabia - with grant number (QU-2023-QU-R-3-1-EI-12975).

Consent to participate

All Authors concur with the submission. The corresponding Author is responsible for ensuring that the descriptions are accurate and agreed by all authors. The work has not been published elsewhere, either completely, in part, or in another form. The manuscript has not been submitted to another journal and will not be published elsewhere. Publication in any reasonably retrievable source constitutes prior publication.

Authors' contribution

Conceptualization: All authors contributed to the study's conception and design. All authors analyzed and interpreted the data. All authors wrote the first draft of the manuscript. All authors revised and approved the final manuscript.

Competing interests

There is no conflict of interest.

Availability of data and materials

Meeting abstracts or preprints as well as academic theses do not constitute prior publication.

REFERENCES

1. Tazmeen, T. Mir F.Q. Sustainability through materials: A review of green options in construction. *Results Surf. Interfaces* **2024**, 14, 100206.
2. Pandey, J.; Takagi, H.; Nakagaito, A.; Kim, H. *Handbook of Polymer Nanocomposites. Processing, Performance and Application*, 1st ed., Heidelberg: Springer; **2015**; p 27-36.
3. Thakur, V.K. *Nanocellulose Polymer Nanocomposites: Fundamentals and Applications*. Beverly, 1st ed., MA: John Wiley & Sons; **2015**; p 14-25.
4. Thakur, M.K., Rana, A.K. and Thakur, V.K. *Lignocellulosic Polymer Composites: A Brief Overview.* In Lignocellulosic Polymer Composites, **2014**; p 3-12.
5. Kargarzadeh, H.; Huang, J.; Lin, N.; Ahmad, I.; Mariano, M.; Dufresne, A. Recent developments in nanocellulose-based biodegradable polymers, thermoplastic polymers, and porous nanocomposites. *Prog. Polym. Sci.* **2018**, 87, 197-227.
6. Ragab, T.I.M.; Alminderej, F.M.; El-Sayed, W.A.; Saleh, S.M.; Shalaby, ALG. Enhanced optimization of bioethanol production from palm waste using the SM Taguchi method. *Sustainability* **2021**, 13, 13660.
7. Mohamed, E.M.; Mohammed, A.; AbdulSattar, K.M. Beneficial effects of date palm fruits on neurodegenerative diseases. *Neural Regen. Res.* **2016**, 11, 1071-1072.
8. Bauza, E.; Dal Farra, 1.C.; Berghi, A.,Oberto, G.; Peyronel, D.; Domloge, N. Date palm kernel extract exhibits antiaging properties and significantly reduces skin wrinkles. *Int. J. Tissue React.* **2002**, 24,131-136.
9. Ragab, T.I.M.; Hassan, N.S.Y. A Comparative study between different additives for date pits coffee beverage; health and nutritional evaluation. *Egypt. J. Chem.* **2019**, 777-790.
10. Shen, Y.; Peng, H.; Bi, H. Insight into the physicochemical characteristics and biological features of dietary polysaccharides extracted from palm kernel cake. *Grain Oil Sci. Technol.* **2025**, 8, 77-88.
11. Sheikh, D.M.El.; El-Kholany, E.A; Kamel, S.M. Nutritional value, cytotoxicity, anti-carcinogenic and beverage evaluation of roasted date pits. *World J. Dairy Food Sci.* **2014**, 9, 308-316.
12. Besbes, S.; Blecker, C.; N.D.; Roanne, D.; Attia,H. Date seeds: Chemical composition and characteristic profiles of the lipid fraction. *Food Chem.* **2004**, 84, 577-584.
13. Jassim, S.A.; Naji, M.A. In vitro evaluation of the antiviral activity of an extract of date palm (*Phoenix dactylifera L.*) pits on a *Pseudomonas phage* evid, based complement. *Alternat Med.* **2010**, 7, 57-62.
14. AlAlaw, R.; Alhamdani, M.S.S. J.D. Hoheisel, Y. Baqi, Antifibrotic and tumor microenvironment modulating effect of date palm fruit (*Phoenix dactylifera* L.) extracts in pancreatic cancer. *Biomed. Pharmacother.* **2020**, 121, 1095222.
15. Abdelbaky, A.S.; Tammam, M.A.; Ali, M.Y.; Sharaky, M.; Selim, K.; Semida, W.M.; Abd El-Mageed, T.A.; Ramadan, M.F.; Oraby, H.F.; Diab, Y.M. Antioxidant and anticancer assessment and phytochemical investigation of three varieties of date fruits. *Metabolites* **2023**, 13, 816.
16. Shalaby, A.G.; Ragab, T.I.M.; Mehany, A.B.M.; Helal, M.M.I.; Helmy, W.A. Antitumor and prebiotic activities of novel sulfated acidic polysaccharide from ginseng. *Biocatal. Agric. Biotechnol*. **2018**, 14, 402-409.
17. Ragab, T.I.M.; Amer, H.; Wasfy, A.A.F.; Abdel Hady, M.S.H.; Mossa, A.T.; Liebner, F. Sulfated cellulose from agriculture wastes, anticoagulant, fibrinolytic and toxicological studies. *J. Environ. Sci. Technol.* **2014**, 7, 266-280.
18. Mohammad, M.S.; Farhad, Z.; Fatemeh, D. Date palm wood flour as filler of linear low-density polyethylene. *Composites Part B: Engineering* **2014**, 137-141.

19. Brodeur,G.; Yau, E.; Badal, K. J.; Collier, K.B.; Ramachandran, S.; Ramakrishnan Chemical and physicochemical pretreatment of lignocellulosic biomass: A review. *Enzyme Res.* **2011**, 20-12.
20. Sun, C.K.; Chu, S.W.; Chen, S.Y.; Tsai, T.H.; Liu, T.M.; Lin, C.Y.; Tsai, H.J. Higher harmonic generation microscopy for developmental biology. *J. Struct. Biol.* **2004**, 147, 19-30.
21. Paralikar, K.M.; Aravindanath, S. Crystallization of cellulose. *J. Appl. Polym. Sci.* **1988**, 35, 2085-2089.
22. Ragab, T.I.M.; Shalaby, A.S.G.; El Awdan, S.A.; Refaat, A.; Helmy, W.A. New applied pharmacological approach/trend on utilization of agro-industrial wastes environment. *Sci. Poll. Res.* **2018**, 25, 26446-26460.
23. Sonowal, D., Wani, K.M. Comprehensive review of cellulose nanocrystals: preparation, properties, modifications and applications. *Bull. Natl. Res. Cent.* **2025**, 49, 55-59.
24. Ali, S.E.; Farag, M.A.; Holvoet, P.; Hanafi, R.S.; Gad, M.Z. A comparative metabolomics approach reveals early biomarkers for metabolic response to acute myocardial infarction. *Sci. rep.* **2016,** 16, 36359.
25. Broeckling, C.D.; Reddy, I.R.; Duran, A.L.; Zhao, X.; Sumner, L.W. MET-IDEA: Data extraction tool for mass spectrometry-based metabolomics. *Anal. Chem.* **2006**, 78, 4334-4341,
26. Thygesen, A.; Oddershede, J.; Lilholt, H.; Thomsen, A.B.; Stahl, K. On the determination of crystallinity and cellulose content in plant fibres. *Cellulose* **2005**, 12, 563-576.
27. Ragab, T.I.M.; Wasfy, A.A.F.; Amer, H.; El-Gendi, A.; Abdel Hady, M.S.; Liebner, F. Synthesis of cellulose acetate membrane from the Egyptian rice straws. *J. Appl. Sci.* **2014**, 14, 3424-3435.
28. Rahman, R.; Xu, W.; Jin, H.; Rosbash, M. Identification of RNA-binding protein targets with Hyper TRIBE. *Nat. Protoc.* **2018**, 8, 1829-1849.
29. Rosa, A.C.; Rattazzi, L.G.; Miglio, C.M.; Fantozzi, R. Angiotensin II induces tumor necrosis factor-α expression and release from cultured human podocytes. *Inflamm Res.* **2012**, 61, 311-317.
30. Hazwan, H.N.; Aqilah, M.; Zaharaddeen, P.; Garb, N.; Jain, K.M.; Abdul Rahim,A.; Nicols, B.; Mehdi Yemloul, M.R.; NurulFazita, M.K.; Mohamad, H. Physicochemical of microcrystalline cellulose from oil palm fronds as potential methylene blue adsorbents. *Int. J. Biol. Macromol.* **2016**, 92, 11-19.
31. Pallab, K.; Barman, T.K.; Pal Tapas, K.; Ramen, K. Estimation of total flavonoids content (TFC) and antioxidant activities of methanolic whole plant extract of *Biophytum sensitivum* Linnal. *J. Drug Deliv. Ther.* **2013**, 3, 33-37.
32. Ibrahim, M.M.; Ali, H.M.; Abdullah, M.A.; Hassandarvish, P. Acute toxicity and gastroprotective effect of the Schiff base ligand (1)Hindole-3-ethylene-5-nitrosalicylaldimine and its nickel (II) complex on ethanol induced gastric lesions in rats. *Molecules* **2012**, 17, 2449-12459.
33. Ciolacu, D.; Ciolacu, F.; POPA, V.I. Amorphous cellulose – structure and characterization. *Cellulose Chem. Technol.* **2011**, 45, 1-2.
34. De Man, J.D; Rogosa, M; Sharpe, M.E. A medium for the cultivation of lactobacilli. *J. appl. Bact.* **1960**, 23, 130-135.
35. Pepeljnjak, S.; Kalodera, Z.; Zovko, M. Investigation of antimicrobial activity of *Pelargoniumradula*(Cav.) *L'Hérit. Acta Pharma.* **2005**,55, 409-415.
36. Shalaby, A.G.; Ragab, T.I.M.; Mehany, A.B.M.; Helal, M.M.I.; Helmy, W.A. Antitumor and prebiotic activities of novel sulfated acidic polysaccharide from ginseng. *Biocatal. Agric. Biotechnol.* **2018**, 14, 402-409.
37. Shalaby, A.L.G.; Esawy, M.A.; Hussien, M.M. Comparative study between free and immobilized *Penicillium chrysogenum* mannanase: A local fungal isolate. *J. Appl. Pharm. Sci.* **2017**, 7, 97-104.

38. Hwang E.S.; Thi, N.D. Effects of extraction and processing methods on antioxidant compound contents and radical scavenging activities of laver (Porphyratenera) preventive. *Nutr. Food Sci.* **2014**, 19, 40-8.
39. Thabrew, M.I.; Hughes, R.D.; McFarlane, I.G. Screening of hepatoprotective plant components using a HepG2 cell cytotoxicity assay. *J. Pharm Pharmacol.* **1997**, 49, 1132-1135.
40. El-Menshawi, B.S.; Fayad,W.; Mahmoud, K.; El-Hallouty, SM.; El-Manawaty, M.;Olofsson, MH.; Linder, S. Screening of natural products for therapeutic activity against solid tumors. *Indian J. Exp. Biol.* **2010**, 48, 258-264.
41. Shawky, B.T.; Ragab, T.I.M.; Hussein, H.M.; Zahran, M.K. Optimization of cellulolytic enzymes production from local potent fungi using full factorial design for bioethanol production from MFEX-treated rice straw using Klebsiellaoxytoca P2. *Biosci. Res.* **2018**, 15, 250-261.
42. Degnan, B.A.; Macfarlane, G.T. Transport and metabolism of glucose and arabinose in Bifidobacteriumbreve. *Arch. Microbiol.* **1993**, 160,144-151.
43. Freeze, H.H.; Sharma, V. Metabolic manipulation of glycosylation disorders in humans and animal models. *Semin. Cell Dev. Biol.* **2010**, 21, 655-662.
44. Lima, M.M.; Borsali, R. Rodlike cellulose microcrystals: Structure, properties and applications. *Macromol. Rapid. Commun.* **2004**, 25, 771-787.
45. Thygesen, A.; Oddershede, J.; Lilholt, H.; Thomsen, A.B.; Stahl, K. On the determinaion of crystallinity and cellulose content in plant fibres. *Cellulose* **2005**, 12, 563-576.
46. Abd El-Rahman, S.N.; Al-Mulhem, S.I. Characteristic analysis, antioxidant components and antioxidant activity of date fruits, date seeds and palm ShellClin. *Med. Case Rep.* **2017**, 1, 1.
47. Juhaimi, F.A.; Ghafoor, K.; Özcan, M.M. Physical and chemical properties, antioxidant activity, total phenol and mineral profile of seeds of seven different date fruit (*Phoenix dactylifera* L.) varieties. *Int. J. Food Sci. Nutr.* **2011**, 63, 84-89.
48. Tariq, M.; Batool, A.; Abbas, N.; Hussain, A. Synthesis, characterization, anti-microbial and cytotoxic applications of zinc(II) complexes. *Bull. Chem. Soc. Ethiop.* **2021**, 35, 287-299.
49. El-Beltagi, H.S.; Aboelftoh, A.; Ahmed, A.R.; Wahdan, K.M.; Elkatary, H.O.; Osman, A.; Ismail, A.M.; Abo El-Maati, M.F. Bioactive potential of lemon leaves: Antioxidant, antiproliferative, and antimicrobial activities. *Bull. Chem. Soc. Ethiop.* **2026**, 40, 1185-1204.